AGU PUBLICATIONS

Journal of Advances in Modeling Earth Systems

RESEARCH ARTICLE

10.1002/2016MS000625

Calibration-induced uncertainty of the EPIC model to estimate climate change impact on global maize yield

Wei Xiong[1,2], Rastislav Skalský[3,4], Cheryl H. Porter[2], Juraj Balkovič[3,5], James W. Jones[2], and Di Yang[1]

[1]Climate Change Division, Institute of Environment and Sustainable Development in Agriculture, Chinese Academy of Agricultural Sciences, Beijing, China, [2]Department of Agricultural and Biological Engineering, University of Florida, Gainesville, Florida, USA, [3]International Institute of Applied Systems Analysis, Ecosystem Services and Management Program, Laxenburg, Austria, [4]National Agricultural and Food Centre, Soil Science and Conservation Research Institute, Bratislava, Slovak Republic, [5]Faculty of Natural Sciences, Comenius University in Bratislava, Bratislava, Slovak Republic

Key Points:
- Tuning-specific parameters improve spatial agreement to reported maize yield
- Calibration leads to a modest bias for climate change projections for the globe
- Calibration leads to pronounced difference in some locations, highlighting the adaptation

Supporting Information:
- Supporting Information S1

Correspondence to:
W. Xiong,
wei.xiong@ufl.edu or
xiongwei8848@hotmail.com

Citation:
Xiong, W., R. Skalský, C. H. Porter, J. Balkovič, J. W. Jones, and D. Yang (2016), Calibration-induced uncertainty of the EPIC model to estimate climate change impact on global maize yield, *J. Adv. Model. Earth Syst.*, *8*, doi:10.1002/2016MS000625.

Received 4 JAN 2016
Accepted 2 AUG 2016
Accepted article online 5 AUG 2016

Abstract Understanding the interactions between agricultural production and climate is necessary for sound decision-making in climate policy. Gridded and high-resolution crop simulation has emerged as a useful tool for building this understanding. Large uncertainty exists in this utilization, obstructing its capacity as a tool to devise adaptation strategies. Increasing focus has been given to sources of uncertainties for climate scenarios, input-data, and model, but uncertainties due to model parameter or calibration are still unknown. Here, we use publicly available geographical data sets as input to the Environmental Policy Integrated Climate model (EPIC) for simulating global-gridded maize yield. Impacts of climate change are assessed up to the year 2099 under a climate scenario generated by HadEM2-ES under RCP 8.5. We apply five strategies by shifting one specific parameter in each simulation to calibrate the model and understand the effects of calibration. Regionalizing crop phenology or harvest index appears effective to calibrate the model for the globe, but using various values of phenology generates pronounced difference in estimated climate impact. However, projected impacts of climate change on global maize production are consistently negative regardless of the parameter being adjusted. Different values of model parameter result in a modest uncertainty at global level, with difference of the global yield change less than 30% by the 2080s. The uncertainty subjects to decrease if applying model calibration or input data quality control. Calibration has a larger effect at local scales, implying the possible types and locations for adaptation.

1. Introduction

Crop growth modeling has increasingly been applied at large spatial scales, such as country, continent, and global. These simulation effects are driven by the increasing needs to evaluate the impacts of climate change on food production [*Balkovič et al.*, 2014; *Deryng et al.*, 2014], understand yield gaps and food security [*Van Wart et al.*, 2013], devise adaptation options [*Challinor et al.*, 2014], identify risk management strategies [*van der Velde et al.*, 2014], and incorporate crop models to integrated assessment for policy implications [*Ewert et al.*, 2011]. For these purposes, some crop models are designed to represent key biophysical processes between environment, management, and crop, and to be applicable in simulating over large areas. For instance, with the availability of a suite of global data sets (i.e., crop planting and harvesting dates, fertilizer, area), the GLAM [*Challinor et al.*, 2004], PEGASUS [*Deryng et al.*, 2011], and iGAEZ [*Tatsumi et al.*, 2011] models were created to assess the impacts of climate change on global food production. On the other hand, to better represent spatial heterogeneity of agricultural management and crop genotypes, many process-based and site-specific crop models have also been used for large-scale simulations. These models include detailed crop management options and crop physiology characteristics, and necessitate substantial amounts of data to calibrate the model for a particular region. For example, *Elliott et al.* [2014] developed a global gridded crop simulation system (pSIMS) based on crop models DSSAT [*Jones et al.*, 2003] and APSIM [*Keating et al.*, 2003]. The EPIC model, developed to assess the effect of soil erosion on productivity in agricultural management, has been upscaled to simulate global crop production, using a Geographic Information System (GIS) [*Liu et al.*, 2007].

Although a wide range of models have been used to forecast global yield response to environment and management changes, the magnitude, direction, and pattern of the responses have differed to

such an extent that cross-study syntheses are restricted and the ability to devise relevant adaptation options and develop risk management strategy are limited [*Challinor et al*., 2014; *Rosenzweig et al*., 2013]. One source of the uncertainties comes from the differences between models, particularly in structure and process. *Rosenzweig et al*. [2014] compared global inferred yield change under the same set of climate change drivers from seven global gridded crop models. They found substantial disparity in estimated direction, rate, and pattern of yield responses to climate warming. Other studies compared the uncertainties due to crop models in a number of sites. For example, *Asseng et al*. [2013] conducted the largest standardized model intercomparison to date for climate change impact, by comparing 26 wheat models. *Bassu et al*. [2014] compared 23 maize models regarding the simulated yield responses to changes in climatic factors. Due to the large uncertainty, most of these studies concluded that an ensemble of models increases the applicability of the multiple simulation results. But on the other hand they also pointed out a comprehensive calibration with detailed observed data set tends to decrease the range of estimation and therefore reduce the uncertainty, highlighting the importance of model calibration.

Another source of uncertainty relates to model inputs. Recently the Global Gridded Crop Model Intercomparison (GGCMI) project was initiated within the framework of the Agricultural Model Intercomparison and Improvement Project [*Elliott et al*., 2015; *Rosenzweig et al*., 2013]. One of the goals of the project was to reduce and quantify the uncertainty among models by harmonizing their inputs (e.g., global crop area, nutrients, irrigation, crop planting, and harvesting calendar) and providing consistent simulation protocols. The availability of the global data sets provides great opportunity for process-based global crop simulation. Many groups have used these data sets to setup their global models and made simulations (e.g., GEPIC, LPJmL). However, these global data products usually derive from survey, remote sensing, country-level data, or expert judgment, which can be subject to large errors, particularly in areas where the crop is a marginal product or areas without good data collection infrastructure. For example, the global fertilizers and manure data set [*Müeller et al*., 2012] provides uniform values for some large areas or countries, particularly in the developing world, exhibiting much less heterogeneity than that of reported yields and tending to decrease the correlation between simulated and reported yields. Additionally, the variables contained in the global data sets are far below the requirements of most process-based crop models. Current global data sets only provide coarse information of crop area, the total amount of fertilizer, and manure applied on crops, crop planting, and harvesting windows, and these data are usually only available for certain years (such as year of 2000). Whereas for a precise crop simulation, much more detailed data such as crop phenology, exact dates of planting, and management information are needed. The lack of sufficient data to run the models lead to equivocal selection of many model parameters, enabling calibration as a useful way to improve the simulation.

Model calibration is a prerequisite step for crop simulation. For site-scale simulation, it is commonly operated through the adjustment of specific parameters to match the field observations. While at regional scale, particularly the global simulations, this step is usually simplified or ignored owing to the lack of observed data. One frequently used calibration strategy for global simulations involves apply default parameters universally while adjusting a few based on literatures [e.g., *Balkovič et al*., 2013], or varying parameters based on the relationship between climate and crop phenology [e.g., *Elliott et al*., 2014; *Waha et al*., 2012]. Another common method is to repeat the simulation with different parameters (such as planting dates) and then select the parameters that reach a given criterion (e.g., highest yield) [e.g., *Liu*, 2009]. A more complex method is to calibrate selected parameters based on observation, survey, and reported regional data, which requires much more computation time. For example, *Folberth et al*. [2012] calibrated cultivar, planting dates, and tillage parameters in EPIC to reflect the local agricultural practices of low input, low-yielding cultivar, and high nutrient depletion in Sub-Saharan Africa, and therefore produced a better agreement of simulation to reported maize yield. Based on spatially distributed experimental observations, *Xiong et al*. [2008] used a cross-calibration method to calibrate seven cultivar and three management parameters of DSSAT in China, substantially increased the agreement between simulation and survey maize yields from 1981 to 2000. Nevertheless, with the increasing efforts to regionalize or calibrate model parameters for better global simulations, questions related to calibration are largely remained unclear, including (1) the magnitude of the uncertainty related to global crop simulation using harmonized global data sets as input, including simulation differences between default and tuned model

parameters, and (2) the possible effects of calibration on simulation results for climate change impact assessment.

The aim of this study therefore was to apply the harmonized global data sets on the EPIC model, for both setting up the global maize simulation and regionalizing the parameters. It also attempted to quantify the uncertainty due to different values of model parameter and calibration. The fundamental goal of the study was to understand the possible uncertainty range due to model calibration on estimated impacts of climate change, facilitating robust yield projection for adaptation investment, and policy making.

2. Method

2.1. The EPIC Model

We used the EPIC model (Ver. 0810) [*Williams*, 1995], one of the most widely used crop models, to simulate the global maize production and quantify the projected range of climate change impact under different calibration strategies. The model has been utilized to simulate soil carbon sequestration [*Zhang et al*., 2015], management practices [*Lychuk et al*., 2014], nutrient cycling and loss [*Wang et al*., 2006], and climate change impact on crop yield [*Balkovič et al*., 2014]. Because the model is open source software written in FORTRAN programming language, we modified it for parallel processing in a Linux environment and to make it capable of iterative simulations over a large number of parameter settings. Although EPIC has a relatively simple model structure compared to other process-based crop models like APSIM and DSSAT, it comprises most of the major processes that occur in the soil-water-atmosphere-management system, such as water dynamics, cycling of nitrogen and phosphorus, soil salinity, and aluminium toxicity.

EPIC operates on a daily time step and can perform long-term simulations. It has eight major modules: weather generation, crop growth, soil water dynamics, erosion, nutrient and carbon cycling, soil temperature, tillage, and crop and soil management. In the crop growth routine, crop yield is estimated as a function of the biomass to energy ratio (BE), the harvest index (HI), planting density (SD), photosynthetic active radiation (PAR), radiation use efficiency factor (RUE), and vapor pressure deficit (VPD), and is reduced through a series stress factors. Potential biomass is calculated daily from PAR and RUE. Potential biomass is adjusted to actual biomass through daily stress caused by extreme temperatures, water, and nutrient deficiency or inadequate aeration. Then, crop yield is calculated as a proportion of economic yield over total actual above-ground biomass at maturity defined by a harvest index. The total number of model input parameters is more than 300, most of them associate to specific type of crop and agricultural management regime, but values of a few model inherent parameters such as Potential Heat Unit (PHU), Optimum Temperature (OT), Harvest Index (HI) need to be optimized with respect to circumstances in specific study region and crop cultivar. Based on previous sensitivity analyses of EPIC [*Xiong et al*., 2014], we selected four parameters to be adjusted in the simulation, i.e., PHU, OT, HI, SD, respectively, representing spatial heterogeneity of crop phenology, biophysical characteristic, yield formation, and management.

2.2. Global EPIC Simulation

In this study, maize was chosen as the target crop to quantify the uncertainty of calibration. Maize is one of the most important staple crops in the world, with relatively good information on yield, area, and management. The data used for the EPIC model include topography, land cover, weather, soil, management, and plant parameters. We collected the most complete data sets on climate, soil, topographic relief, and crop management from different public sources and converted them to simulation grids at a resolution $0.5^\circ \times 0.5^\circ$ (supporting information Table S1). We used these to set up a grid-based modeling system for the EPIC, v. 0810 model. The global modeling system was constructed by combining GIS layers on soil, relief, management, and weather grid [*Balkovič et al*., 2013; *Xiong et al*., 2014], with around 40,000 simulation units of cropland upon which the EPIC model was run.

Six daily weather variables (maximum and minimum temperatures, precipitation, solar radiation, relative humidity, and wind speed) for the period 1951–2010 (baseline time period) were obtained from a high-resolution global data set at Princeton University [*Sheffield et al*., 2006] and mapped to the simulation grid cells. This historical weather database was constructed by combining a suite of global observation-based data sets with the National Centers for Environmental Prediction-National Center for Atmospheric Research (NCEP-NCAR) reanalysis, with a geographical resolution of 1.0°. For future climate, we used the HadGEM2-ES

Table 1. Calibration Strategy for the Global Simulation

No	Strategy	Parameters Being Adjusted	Adjusting Range
1	Default	N/A	The middle points of sowing and harvesting window
2	PHU	Potential heat unit and sowing and harvesting date	An incremental increase of 10 days within the sowing and harvesting windows
3	HI	Harvest index	0.3∼0.8 with a step 0.05
4	OT	Optimum temperature	23∼30 with a step of 0.5
5	SD	Sowing density	3∼10 with a step 1

climate change projection using Representative Concentration Pathway 8.5 (RCP8.5), which indicates a climate with radiative forcing more than 8.5 W m^{-2} and a concentration of more than 1370 ppm CO_2-equiv. in 2100. The climate scenario data from the HadGEM2-ES model [*Collins et al*., 2008] was retrieved from CMIP website (http://cmip-pcmdi.llnl.gov/cmip5) and was bias-corrected with respect to historical observations by *Hempel et al*. [2013] to remove systematic errors.

Topographic data were obtained from the global 30″ digital elevation model (DEM) (GTOPO30), a 1 km resolution data set made available by the United States Geological Survey (USGS). The high-resolution global Shuttle Radar Topography Mission DEM from NASA [*Farr et al*., 2007] in 3′ spatial resolution was used as a source for calculation of slope data.

Soil parameters (soil texture, bulk density, pH, organic carbon content, and fraction of calcium carbonate for each of five 20 cm thick soil layers) were obtained from International Soil Profile Data set (WISE) [*Batjes*, 1995]. Soil parameters were allocated to each simulation grid cell based on the spatially dominant soil type taken from the digital Soil Map of the World (DSMW) [*FAO*, 1990]. Soil retention and hydraulic parameters were calculated using pedotransfer functions [*Schaap and Bouten*, 1996]. Soil parameters for organic soils missing in WISE data set were adopted from *Boogaart et al*. [1998]. The 5′ spatial resolution model on global cropland land uses [*You and Wood*, 2006] served as a source of cropland extent data.

Crop yields and harvesting areas came from the gridded global data set by combining two data products of *Monfreda et al*. [2008] and Spatial Production Allocation Model (SPAM) [*You et al*., 2009], reflecting the production situations around 2000s. The crop calendar data set was obtained from the Center for Sustainability and Global Environment (SAGE). This data set is the result of digitizing and georeferencing existing observations of crop planting and harvesting dates, at a resolution of 5′ [*Sacks et al*., 2010]. The data set provides ranges of crop planting and harvesting dates for different crops in each grid. A crop-specific gridded data set (by 5′) of nitrogen, phosphorus, and potash fertilizer application for the world (around the years of 1999 or 2000) was used in our simulation to setup current fertilizer application rate for maize in each grid cell. This data set was developed by University of Minnesota, based on a spatial disaggregation method to fuse both national and subnational fertilizer application data from a variety of sources [*Müeller et al*., 2012].

2.3. Calibration Strategy

The lack of information on spatial distribution of maize cultivars and cropping practices necessitated the calibration in our EPIC modeling. Calibration is the common method to reduce the simulation bias. At the global scale, this procedure is usually fulfilled through regionalization of selected parameters. Here we conducted the global simulation with five calibration strategies (Table 1):

1. The Default Simulation. This indicates a single global simulation for both irrigated and rainfed maize, directly driven by the global data sets and model default parameters. Sowing dates and the length of growing season were obtained from *Sacks et al*. [2010] (using midpoint dates of the reported windows). The PHU (in °C) was estimated for each grid cell based on Princeton historical weather data (1981–2010), assuming the minimum and optimal growth temperatures of respectively 8°C and 25°C. The harvest operations were automatically postponed by the model if the required PHU had not been accumulated on the given day. The automatic harvest was then triggered at 110% of PHU to take maize postmaturity drying on the field into account. Planting density was set to 5 plant/m^2. HI and OT were the model default values of 0.5Mg·Mg^{-1} and 25°C, respectively.
2. The PHU Simulation. This is the largest simulation group with more than 100 time simulations for each grid cell. We conducted the simulation with default parameters except PHU and associated sowing and

harvesting dates. For each grid, we reiterated the simulation for a number of combinations of sowing and harvesting dates and associated PHU. In the iteration the sowing and harvesting dates changed from the first to the last dates base on their reported windows, with a step of 10 days. PHU was calculated from the observed daily weather data from 1981 to 2010. We selected the PHU and exact planting and harvesting dates for each grid cell that reached the best match between simulated average (1981–2010) and reported mean yields of 2000s and identified as the calibrated values. For exploring the uncertainty due to this calibration, we aggregated global maize yields from the simulations for 25 cultivar maturity types and associated calendar (five sowing dates × five harvesting dates of earliest, early, middle, late, latest), and compared their difference.

3. The HI Simulation. This simulation group repeated the gridded simulation with default parameters, except with different harvest index, from 0.3 to 0.8 Mg, with a step of 0.05 $Mg \cdot Mg^{-1}$. Calibrated parameters were the regionalized HI that minimized the simulation bias. Global maize yields with various HI were averaged, weighted with reported maize area in 2000.
4. The OT Simulation. Same simulation group as the HI simulation, but adjusted the parameter of Optimum Temperature from 23 to 30°C, with a step of 0.5°C. We identified the calibrated OT parameters and computed the global yields for different OT values.
5. The SD Simulation. Same as the simulation group 4 but varied the parameter of sowing density. The SD changed from 3 to 10 plant/m^2, with an incrementally increase of 0.5. The regionalized SD achieved the best spatial agreement to reported yield was considered as calibrated parameters. In addition, global yields were estimated for all SD values.

All the simulations were conducted for the whole global arable land for irrigated and rainfed maize from 1951 to 2099. Area for irrigation was estimated based on the MIRCA2000 database. Since information on the volume of irrigation water supplied is lacking at the global scale, we used the automatic irrigation trigger in EPIC to supply water when the water stress exceeded 20% on a given day, with a maximum annual volume of 1000 mm [*Balkovič et al*., 2014]. Annual N, P, and K fertilizer were applied as rigid amounts together with tillage, while N dosing was triggered automatically based on plant requirements until the annual N application rate indicated by global fertilizer database was reached.

2.4. Analysis

We first evaluated the effectiveness of the calibration strategies for improving the global simulation. This was done by comparing the simulated to historical yields at both country and grid levels. Due to the lack of soil initial condition, we started the simulation from the year of 1951, with a 30 year period (1951–1980) as the spin-up run to reach equilibrium of soil carbon and nutrients [*Balkovič et al*., 2013, 2014]. The average maize yields for each country from 1981 to 2010 were aggregated from gridded outputs, weighted by the reported maize area around 2000. The national yields were compared with FAOSTAT data, in which technology effects in FAOSTAT yields were removed through a linear detrending method to production situations of year 2000 [*Xiong et al*., 2014]. A total of 132 countries with complete reported yields from 1981 to 2010 were selected for the comparison. At grid level, simulated yields (irrigated and rainfed) were compared to SPAM data in terms of the agreement in geographical pattern. Statistics of coefficient of determination (R^2) and relative root mean square error (RMSE) were used to evaluate the effectiveness of the strategies.

We then estimated the uncertainty due to different values of parameters in projecting the impacts of climate change under the scenario of HadGEM2 RCP 8.5. Mean, median, direction (yield increase or decrease), range (difference between highest and lowest values) of the projections in each simulation group were calculated to measure the uncertainty. At the global scale, the PHU simulation with a combination of five sowing (i.e., the earliest, early, middle, later, latest in the sowing window) and five harvesting dates (i.e., the earliest, early, middle, later, latest in harvesting window) were selected and aggregated, representing 25 suites of regionalized parameters (planting and PHU). Simulations of HI, OT, and SD were aggregated with globally identical values of the parameters from lowest to highest. Yield changes were calculated for three periods (2020s: 2011–2039, 2050s: 2040–2069, 2080s: 2070–2099), relative to the corresponding means of 1981–2010. At grid scale, we classified the global arable grids into seven categories based on the medians of the yield change ($<-60\%$, $-60\%\sim-30\%$, $-30\%\sim-5\%$, $-5\%\sim5\%$, $5\%\sim30\%$, $30\%\sim60\%$, $>60\%$), to represent climate change susceptible (yield decrease) and benefit (yield increase) areas, and compared between the simulation groups. We also estimated the range and the direction of the yield changes at grid

level for each simulation group, to examine the uncertainty due to using various values of specific parameters.

3. Results

3.1. Simulation of Historical Yield With Default Parameters

The simulated national yields with default parameters exhibited an overall overestimation over the FAOSTAT data, with a significant and higher prediction by 8.4% (t test, $p < 0.01$) averaged across all countries (Figure 1a). Correlation between the simulated and reported national yields was not significant at 99% confidence level, with $R^2 = 0.078$ and RMSE = 80%, indicating the low agreement in spatial patterns between simulated and reported national yields. Yield overestimation occurred in 82 countries, mainly located in developing countries in Africa and Asia, with a mean overestimation by 143%. Fifty countries exhibited yield underestimation, with a mean underestimation by 46.5%. The countries with yield underestimation mainly located in the North America (e.g., The U.S.), Western Europe (e.g., Spain, France), Western Asia (e.g., Turkey and Iran), and southern part of the South America (e.g., Argentina and Bolivia).

Figure 2 presents the spatial distributions of the reported and simulated historical yields for both irrigated and rainfed maize. Highest maize yields were reported in temperate regions at both hemispheres. The midwestern U.S., Western and Central Europe, and Eastern Argentina emerged as the most productive centers for maize cultivation (yield >8t/ha), characterized by temperate climate and highest nutrient input. Maize in Eastern China, India, Eastern Europe, and Western Asia was reported moderate to high yields, especially in areas equipped with irrigation, with yields ranging between 4 and 8 t/ha. Yields in most of the other areas, particularly Africa were relatively low, possibly due to the low inputs and unfavorable climate. The simulation with default model parameters roughly reproduced the patterns of reported yields between regions, but underestimated the reported yields in high productive regions, such as the U.S., Argentina, West Europe, and overestimated the yields in middle to low productive regions, like China, India, Africa, and South America. In addition, the simulation predicted shifted geographical distribution of the reported yields, for example, the simulations moved the world most productive centers from the midwestern U.S. to the southeastern U.S. for both irrigated and rainfed maize.

3.2. Effectiveness of the Calibration Strategies for Improving the Simulation

Figures 1b–1e shows the comparisons between the FAOSTAT with simulated yields with calibrated parameters. Compared to the simulation with default parameters, the simulations with calibrated parameters demonstrated pronounced improvement in reproducing the spatial patterns of FAOSTAT yields. Regionalizing PHU and HI expressed larger effectiveness to increase the agreement than OT and SD. The R^2 between simulated and FAOSTAT yields increased greatly from 0.078 in the default simulation to 0.6 and 0.58, respectively, in the simulations with calibrated PHU and HI (Figures 2b and 2c). RMSE between the simulated and reported yields across all countries decreased nearly half to around 45% for both the simulations with calibrated PHU and HI.

For majority of the simulation cells, calibration for at least one parameter greatly reduced the bias between the simulated and reported yields. If we considered a simulation with biases within ±15% was acceptable, simulations in only 13.3% of the grid cells for irrigated maize and 9.7% for rainfed maize were acceptable in the simulation with default parameter (overall 22,118 grid cells for irrigated maize and 24,012 for rainfed maize included in the simulation), this low proportion led to a flat and skewed normal distributions of the biases for the default simulation in Figure 3. Calibrating model parameter PHU or HI substantially increased the number of the grid cells that exhibited acceptable simulated values. The proportion of the grid cells with biases within ±15% was increased to 33.2% (irrigated) and 27.4% (rainfed) with calibration strategy PHU, and to 41.6% (irrigated) and 33.6% (rainfed) with calibration strategy HI, largely shrinking the widths and raising the peaks of the possibility distributions for both irrigated and rainfed maize (Figure 3). Both the calibration strategies performed well in main maize areas at middle latitude, such as the U.S. Corn Belt, the North China Plain and Northeast China, Southern part of Brazil (supporting information Figures S1c–S1f). Calibrating model parameter OT or SD had less effectiveness to increase the spatial agreement and reduce the simulation error. Compared to the simulation with default model parameters, the simulation with calibrated OT or SD only increased the R^2 by 0.02∼0.07, reduced the RMSE by 4∼9% (Figures 3d and 3e).

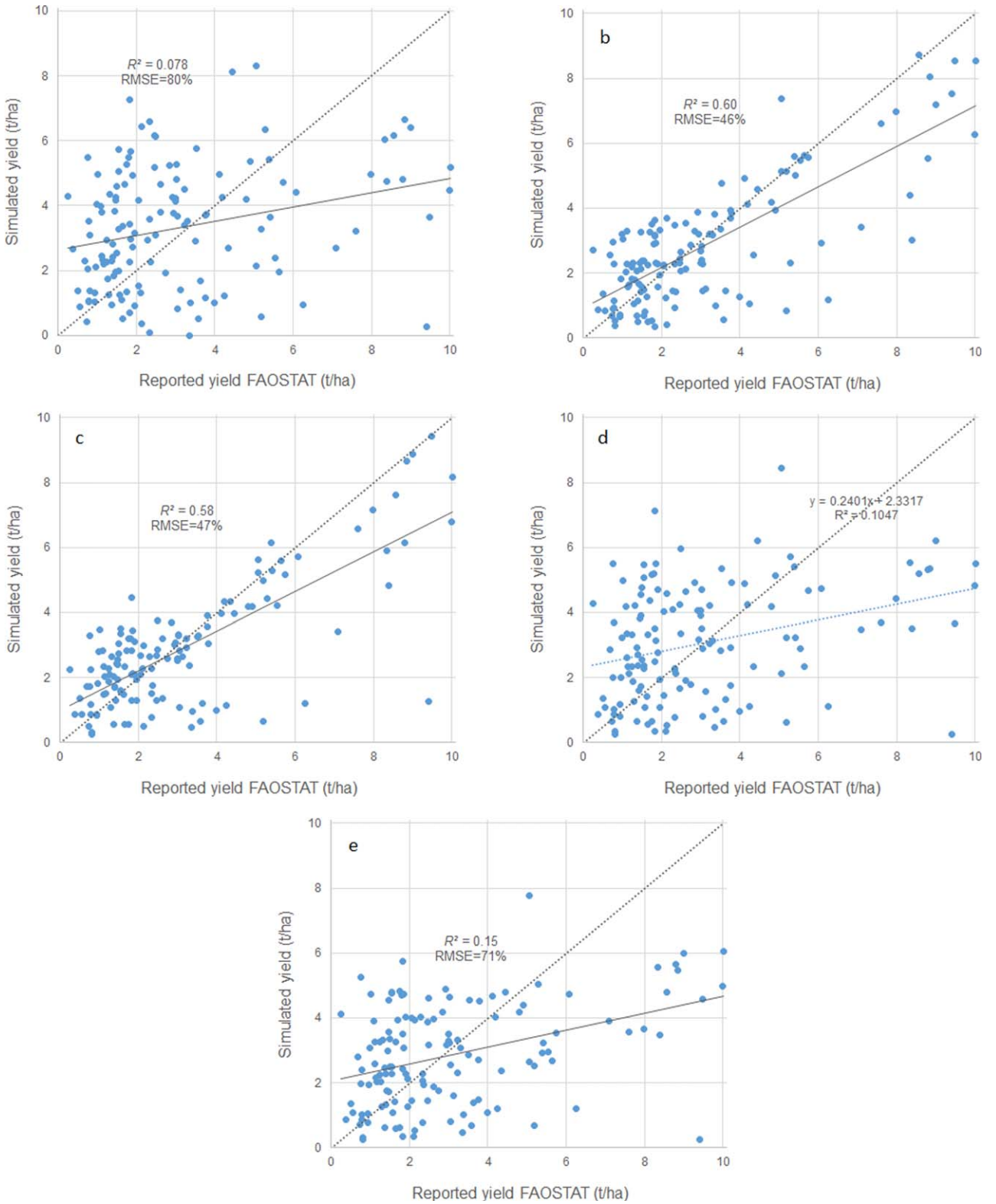

Figure 1. National level comparisons of average yields (1981–2010) between the FAOSTAT data and the simulations with (a) model default parameters, (b) calibrated PHU, (c) calibrated HI, (d) calibrated OT, and (e) calibrated SD.

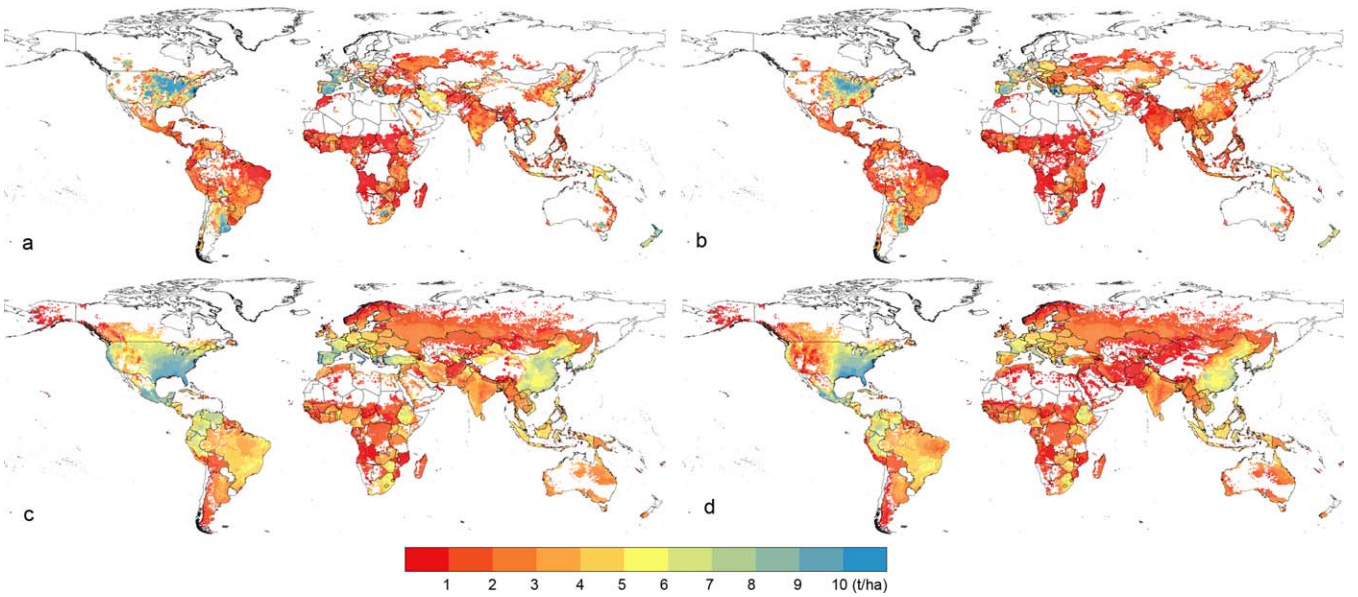

Figure 2. Spatial patterns of reported (2000s) and simulated maize average yields (1981–2010) with model default parameters, (a) reported irrigated yield, (b) reported rainfed yield, (c) simulated irrigated yield, and (d) simulated rainfed yield.

3.3. Estimated Impacts of Climate Change

Model calibration strategies generated slight to wide sensitivities of simulated year-to-year yields when estimating the impacts of climate change, depending on the parameter selected (Figure 4). Varying the HI resulted in the widest yield ranges for the simulated global maize, with average yields of 3.55∼9.14 t/ha for irrigated maize and 1.80∼4.09 t/ha for rainfed maize for the whole simulation period (1981–2099). Adjusting the PHU in the simulation produced the second largest yield ranges in the simulation, with 3.55∼6.30 t/ha and 1.94∼2.94 t/ha, respectively, for irrigated and rainfed maize. Changing the OT or SD has limited influence on simulated yield, particularly for OT. However, whatever the sensitivity that the simulation has, the global yield exhibited a similar downward trend up to 2099 for most calibration strategies, suggesting the consistent negative effects of climate change on global maize production.

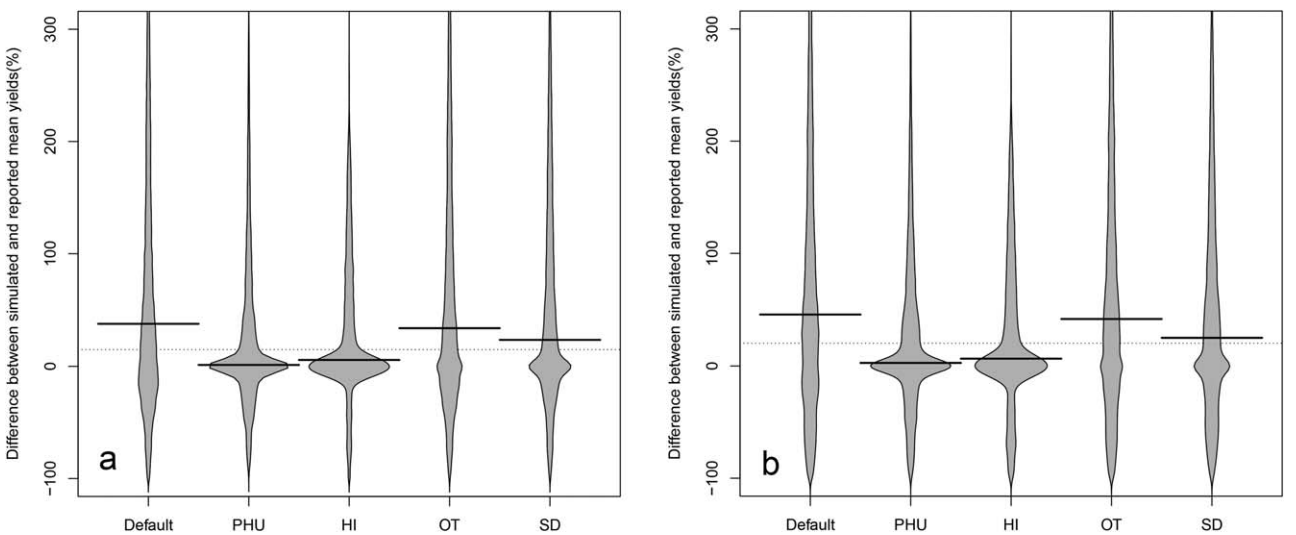

Figure 3. Distribution of the difference between reported and simulated mean yields (1981–2010) with default, one calibrated parameter of PHU, HI, OT, or SD. Difference is converted to the percentage change related to reported mean yield around 2000s (SPAM). The black lines are the medians of the difference for simulation with each calibrated parameter and the dotted lines are the medians for all data sets. (a) Irrigated maize and (b) rainfed maize.

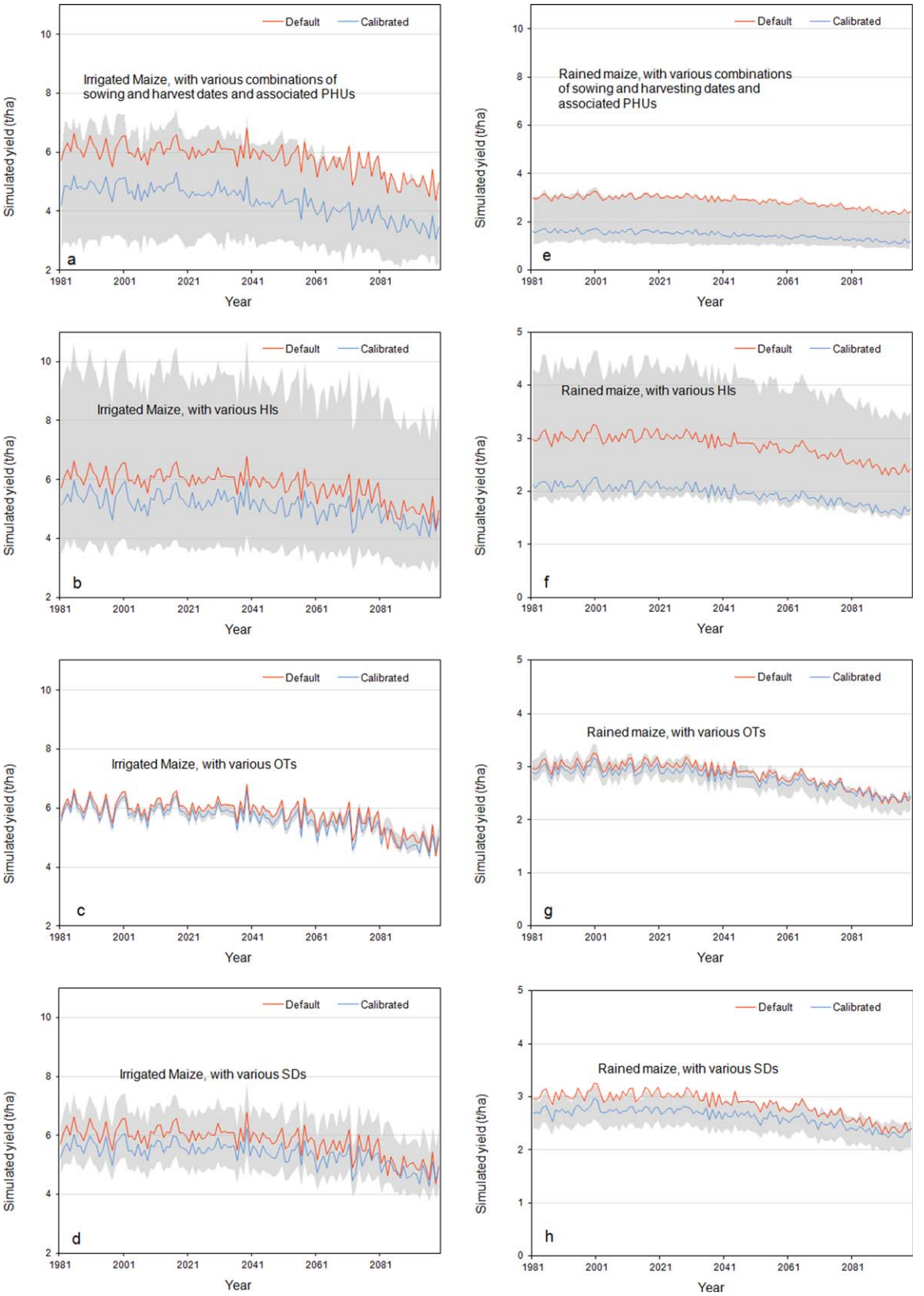

Figure 4. Global maize yields for the simulations with different calibration strategies. Shaded areas indicate the simulation ranges with various parameters. (a–d) Irrigated maize and (e–f) Rainfed maize.

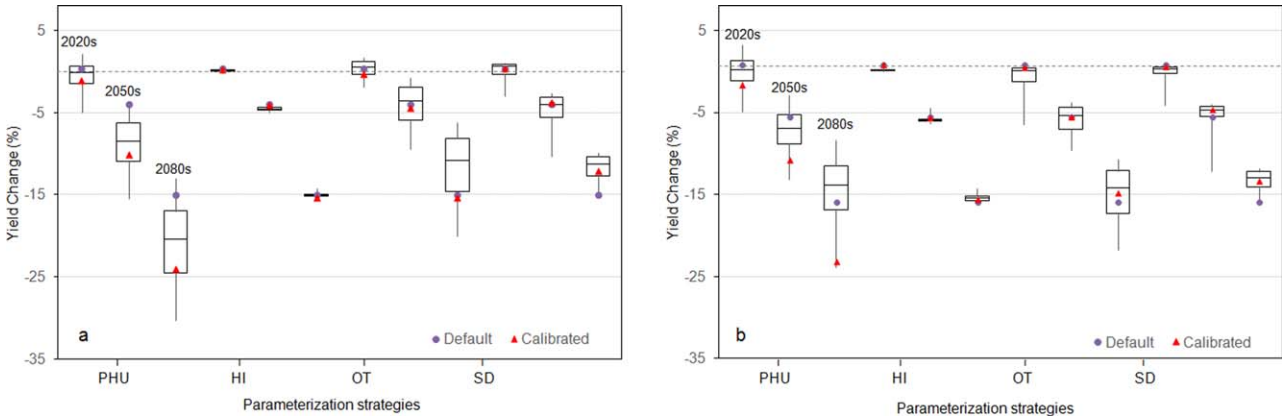

Figure 5. Ranges of estimated yield change with the calibration strategies PHU, HI, OT, and SD, for periods of 2020s, 2050s, 2080s, and RCP85 scenarios. (a) Irrigated maize and (b) Rainfed maize.

Figure 5 and Table 2 present the projected yield changes of the simulations for the three future periods, namely 2020s, 2050s, and 2080s. Under the future climate scenario of RCP8.5 and HadEM2-ES, estimated yield change exhibited largest projection ranges by using different crop phenology, with values of 5.0%∼2.2% (2020s), −15.4%∼−3.5% (2050s), and −30.3%∼−13.0% (2080s) for irrigated maize, and −4.9%∼3.3% (2020s), −13.1%∼−2.9% (2050s), and −23.9%∼−8.3% (2080s) for rainfed maize. That means a difference of 7.7%∼17.3% (the difference between lowest and highest projections at different time periods and conditions) resulted from the strategy for parameterizing PHU, while fixing other parameters at default values. The second largest yield change spread appeared for the calibration strategy OT, with the difference between 3.5%∼13.9%, depending on time periods and irrigation conditions. The strategy of parameterizing SD produced less simulation disparity, with the difference between 4%∼5.2%, while the strategy HI resulted in the least projection difference among simulations with a value less than 2%.

However, although different calibration strategies caused changes to the projections, the difference in estimated global yield change between simulations with default and calibrated parameters were insignificant in most cases. The simulation with default parameters produced a small positive to moderate negative effects on global maize yield due to climate change (RCP 8.5), with yield changes of 0.4% (2020s), −3.9% (2050s), and −15.0% (2080s) for irrigated maize, and 0.9% (2020s), −5.5% (2050s), −16.96% (2080s) for rainfed maize. These estimates were adjusted by −9%∼3.6% if using the parameters that calibrated and regionalized based on the global data sets. Using calibrated PHU in the simulation decreased the estimates in all cases, with an average adjustment −5.1% and the largest −9% for irrigated maize in 2080s. Calibrated HI in the simulation resulted in near zero differences on estimates of future yield change. Employing calibrated OT or SD only resulted in changes in the estimates for the 2080s, with largest adjustment of 3.6% for calibrated parameters SD under rainfed condition.

Table 2. Estimated Yield Changes (%) for Simulations With the Four Calibration Strategies

		Irrigated Maize				Rainfed Maize			
Parameterization Strategy	Period	Mean	Range	With Default	With Calibrated	Mean	Range	With Default	With Calibrated
PHU	2020s	−0.5	−5.0∼2.2	0.4	−1.0	0.0	−4.9∼3.3	0.9	−1.6
	2050s	−8.7	−15.4∼−3.8	−3.9	−10.1	−7.1	−13.1∼−2.9	−5.5	−10.8
	2080s	−20.9	−30.3∼−13.0	−15.0	−24.0	−14.6	−23.9∼-8.3	−16.9	−23.1
HI	2020s	0.1	−0.2∼0.3	0.4	0.3	0.3	0.1∼1.2	0.9	0.9
	2050s	−4.6	−4.9∼−4.3	−3.9	−4.4	−5.7	−6.3∼−4.4	−5.5	−5.6
	2080s	−14.4	−15.6∼−14.2	−15.0	−15.3	−15.4	−16.2∼−14.2	−15.9	−15.6
OT	2020s	0.3	−1.8∼1.7	0.4	−0.2	−1.1	−6.5∼0.6	0.9	0.5
	2050s	−4.2	−9.5∼−0.7	−3.9	−4.4	−6.0	−9.6∼−3.8	−5.5	−5.5
	2080s	−11.8	−20.1∼−6.2	−15.0	−15.3	−15.1	−21.8∼−10.7	−15.9	−14.8
SD	2020s	0.0	−2.9∼1.1	0.4	0.4	−0.3	−4.1∼0.6	0.9	0.6
	2050s	−4.8	−10.3∼−2.6	−3.9	−3.7	−4.4	−12.2∼−4.0	−5.5	−4.6
	2080s	−11.7	−15.0∼−9.8	−15.0	−12.1	−13.3	−15.7∼−11.9	−15.9	−13.3

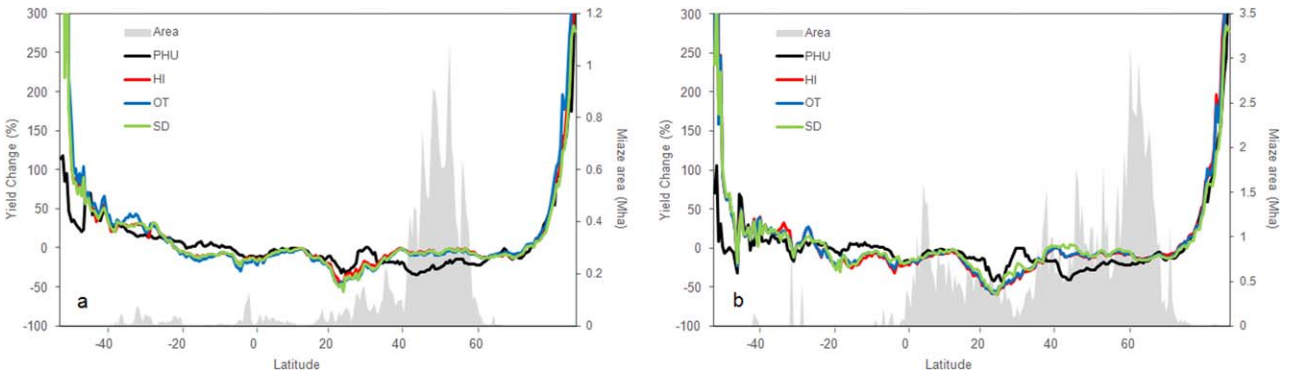

Figure 6. Median of the projected yield changes in 2080s (%) for areas in different latitudes under scenario RCP 8.5 and HadEM2-ES. Lines indicate results of the simulations with different calibrated parameters, shades denote the accumulated maize areas. (a) Irrigated maize and (b) rainfed maize.

3.4. Influence on Identification of Hotspots

Figure 6 presents the aggregated yield change at the 2080s across latitudes for the simulations with the calibrated parameters, in which the medians of the projected changes in all maize grid cells within certain latitudes were used to estimate the yield response curves. Simulations with the four calibrated parameters exhibited a similar pattern of yields responding to climate change, indicated by a negative yield response in low latitude regions while a pronounced yield benefit in regions with high latitude at both hemispheres. The patterns of the yield responses among the simulations with calibrated HI, OT, and SD appeared identical for both irrigated and rainfed maize. Detectable differences occurred in the simulation with calibrated PHU, particularly in the main maize areas. Compared to the simulations with calibrated HI, OT, and SD, inferred median of yield change from the simulation PHU exhibited an increased negative effect in the main maize areas of north hemisphere, while an attenuated negative effect in the main maize areas of low latitude and south hemisphere. Most maize area, particularly the irrigated maize, concentrates in the temperate areas of north hemisphere, spanning from 30°N to 50°N in latitude. In these areas, the simulation with calibrated PHU projected a larger yield susceptibility to climate change than other simulations. The average yield responses in 2080s estimated from the simulation with calibrated PHU in these regions were −23.3% and −25.3% for irrigated and rainfed maize, which were much lower than the simulations with calibrated HI, OT, and SD, respectively, −7.3%, −5.6%, and −6.4% with irrigated maize, and −8.8%, −7.9%, and −5.0 with rainfed maize. There were also disparities between the calibrated PHU simulation and the other simulations in maize areas of south hemisphere and low latitudes of north hemisphere. The simulation with calibrated PHU produced a reduced negative effect or an increased positive effect of climate change in most of these areas.

Heterogeneity of simulated yield response to climate change is often used to identify climate change hotspots for devising adaptation strategies. Here we classified the arable grids into seven categories based on the estimated yield change in 2080s, and identified susceptible and benefit areas for maize production under climate change (Table 3). For maize production under both irrigated and nonirrigation environments, the majority of the grid cells exhibited decreases in yield due to climate change, indicating the widespread negative effects of the global warming on maize. Approximately 50% of the irrigated and 60% of the nonirrigated maize grid cells were identified as susceptible regions with decrease in yield of more than 5%.

Table 3. Number of Grids Identified as Susceptible and Benefited to Climate Change in the 2080s With the Calibration Strategies

Identified Suitability for Maize Production	Index of Yield Change	Irrigated Maize (n = 35,530)				Irrigated Maize (n = 33,214)			
		PHU	HI	OT	SD	PHU	HI	OT	SD
High susceptible	<−60%	5.4	3.5	3.9	3.9	7.6	6.7	6.6	6.1
Middle susceptible	−60%∼−30%	16.7	11.5	9.9	10.7	21.6	16.7	16.0	15.1
Low susceptible	−30%∼−5%	37.1	38.7	39.6	38.3	36.5	36.4	36.5	34.9
Not sensible	−5%∼5%	17.1	21.4	21.7	21.8	15.4	15.4	15.3	16.2
Low benefit	5%∼30%	15.3	15.9	16.0	16.7	16.1	13.2	14.2	15.9
Middle benefit	30∼60%	4.5	5.0	5.0	4.9	4.6	6.3	5.9	6.0
High benefit	>60%	3.9	4.1	3.9	3.7	4.8	5.5	5.5	5.8

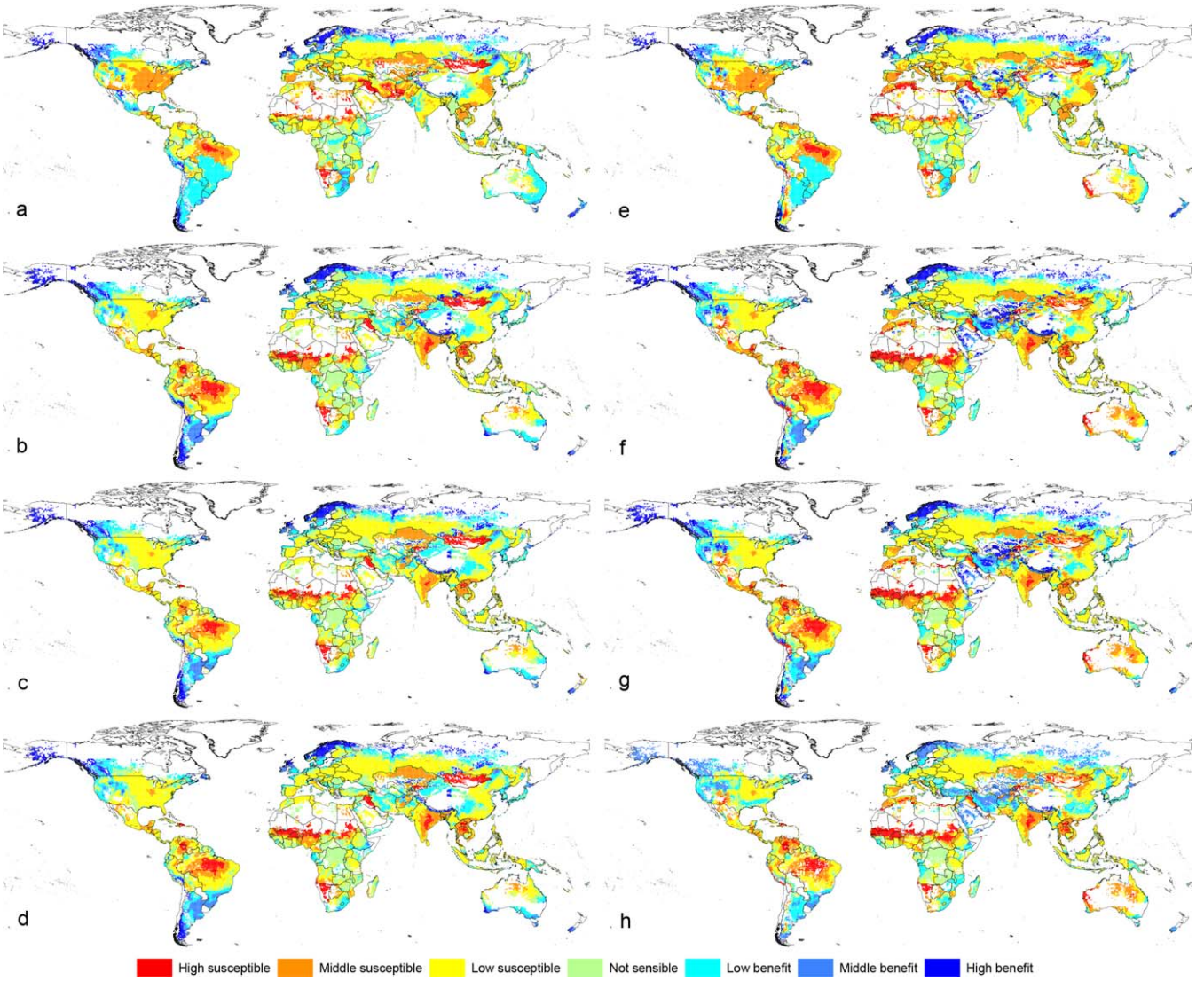

Figure 7. Identified susceptible and benefit areas of maize production to climate change by simulations with the four calibration strategies (PHU, HI, OT, and SD). (a) PHU with irrigation, (b) HI with irrigation, (c) OT with irrigation, (d) SD with irrigation, (e) PHU nonirrigation, (f) HI nonirrigation, (f) OT nonirrigation, and (h) SD nonirrigation.

Around one third of the grid cells appeared middle to high yield susceptibility to climate change, with yield decrease greater than 30%.

Figure 7 presents geographical distributions of the identified susceptible and benefited regions to climate change. For all simulations, grids at high latitudes were projected to benefit from climate change due to current restriction of low growing-season temperatures for maize production. Areas in Central Asian, characterized by high altitude and dry climate, also appeared to benefit from climate change for rainfed maize, possibly due to increased precipitation in the future. For both irrigated and rainfed maize, susceptible areas distributed greatly across geographical regions from latitudes 48°S to 60°N, with a large number of the susceptible areas concentrated in the eastern U.S., Brazil, India, Eastern China, and North of Sub-Saharan Africa. Differences in the identified hotspots were pronounced between the simulations with the four calibration strategies in terms of the size of the susceptible areas and its extent of projected yield decrease. Within the simulations of four calibration strategies, the PHU simulation projected the largest susceptible area and magnitude of yield loss in India and Brazil for both irrigated and rainfed maize, whereas the HI simulation predicted the largest size and extent of susceptibility in the U.S. and China. For Central America (e.g., Mexico), maize yield appeared benefit from climate change in the HI simulation while suffered in other three simulations.

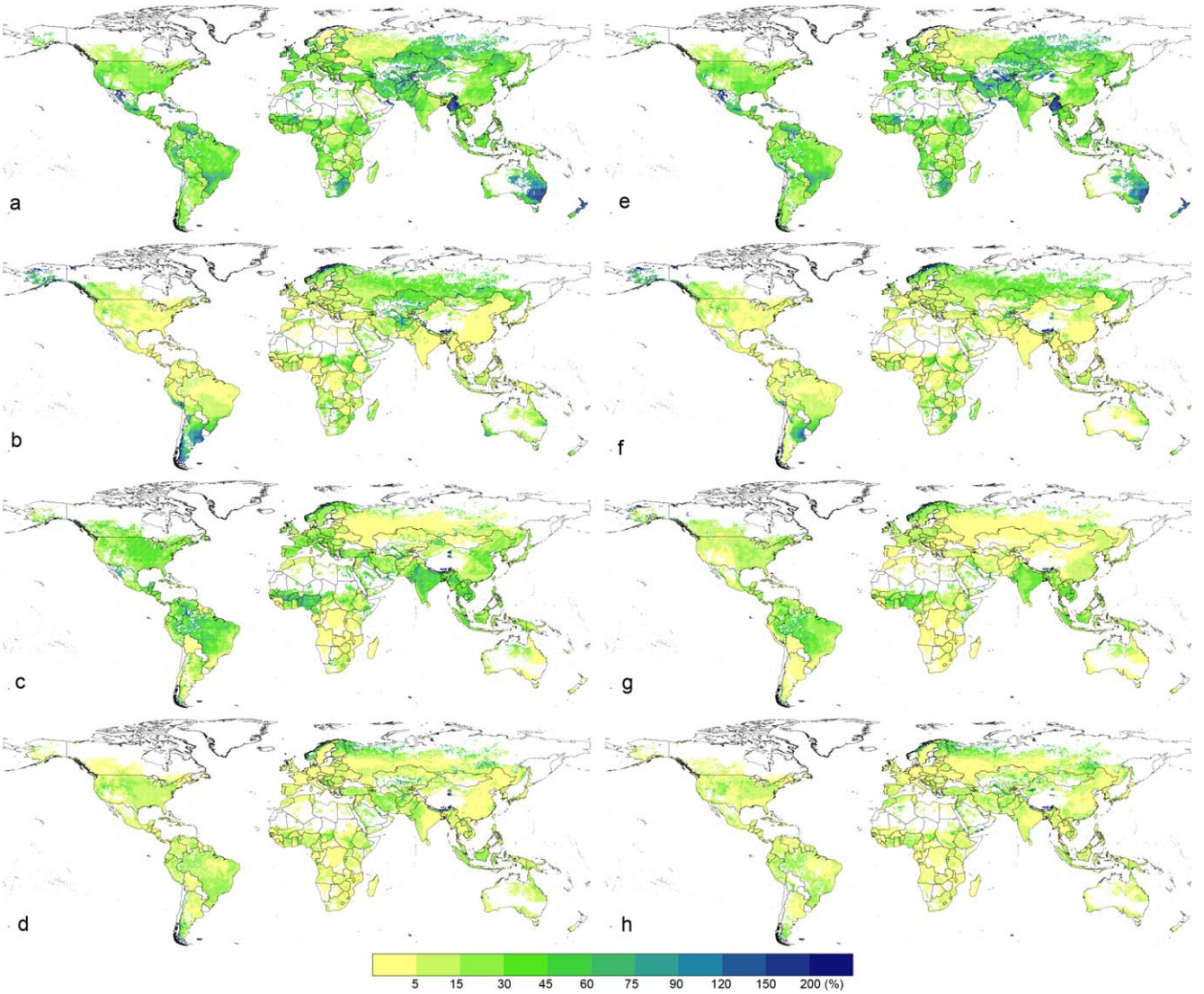

Figure 8. Difference between maximum and minimum projected yield changes within the simulations of different calibration strategies. Dashed areas indicate projections exhibited inconsistent directions. (a) PHU with irrigation, (b) Hi with irrigation, (c) OT with irrigation, (d) SD with irrigation, (e) PHU nonirrigation, (f) HI nonirrigation, (f) OT nonirrigation, and (h) SD nonirrigation.

3.5. Uncertainty due to Calibration

Figure 8 computed the difference of the projected yield responses due to various values of specific parameters in the 2080s to denote the calibration-induced uncertainty. Averaged across all arable grid cells, the differences in projection due to varying model parameter spanned from 14.5% to 37.6%, with largest difference occurred with irrigated maize in the simulation with various PHU, and smallest with rainfed maize in the simulation of different SD. The simulation with different PHU produced the largest uncertainty, indicated by the largest difference of the projections by over 37% for both irrigated and rainfed maize, and the greatest number of grid cells exhibiting contrasting directions, either positive or negative effects in 43.4% irrigated grid cells and 39.7% rainfed grid cells. The median difference of the projections in the simulation PHU was 29% for both irrigated and rainfed maize, suggesting an uncertainty around 30% could be reached if using different PHU setting for the global simulation. In contrast, using difference values of HI, OT, or SD resulted in less simulation uncertainty than that resulted from various settings of PHU. For example, the median difference of the projections in the simulations with varying HI were 8.3% and 7.2%, respectively, for irrigated and rainfed maize, only one fourth of the uncertainty that uses varying PHU. In addition, compared to the simulation PHU, the simulations with varying parameters HI, OT, or SD experienced substantial increase of the number of grid cells that exhibited the difference in projections less than 5%.

Furthermore, parameter-induced uncertainty differed across locations. For example, adjusting PHU and associated crop calendar in the simulation of rainfed maize led to larger uncertainty in countries at low latitude and central Asia, the first 10 countries with the largest projection difference were Myanmar, Oman, Mexico, Uzbekistan, New Zealand, Turkmenistan, Tajikistan, Djibouti, United Arab Emirates, and Armenia. Whereas parameterizing HI caused large uncertainty in countries at high latitude and mountain areas, the first 10 countries with the largest projection difference were Norway, Chile, Sweden, Nepal, Argentina, Bhutan, the U.S., Canada, Qatar, and Latvia (supporting information Table S2).

4. Discussion

4.1. Importance of the Global Data Sets

Like many global simulations [i.e., *Deryng et al*., 2011], our simulation experiment benefits from the development of a suite of global data sets and analyses, including climate, soil, terrain, crop planting and harvesting dates, crop-specific irrigated areas and fertilizer application rates, and harvested areas and yield of major crops. On one hand, these data sets serve as critical gridded inputs for setting up the global simulation. On the other hand, these global data sets provide basic information to calibrate the model, substantially improving the performance of the simulation.

Our simulation without calibration captured only 8% of the spatial variation of historical maize yields across countries. We did not expect the simulation to capture the temporal variation because lack of data to setup the model that reflects the year-to-year changes of important factors. This low agreement partly attributes to model's weakness such as inabilities to simulate the effects of pests, diseases, and extreme events, but also implies the shortcomings of the global data sets for driving the global simulation. Current global data sets are only available for specific temporal resolutions, which is insufficient to parameterize the model to capture the complete variations of yields. For example, in management data sets, the crop calendar reflects practices in the 1990s with wide windows for both sowing and harvesting dates (usually ranging 2 months), fertilizer data only reflects the application practice of 2000s (supporting information Table S1). With the rapid improvement of agricultural technology and unprecedented climate warming rates, these static inputs partly reduce the ability of the simulations to capture the temporal variation of agricultural management. Also data sets like maize fertilizer application rates, maize area and yield, and irrigated area are collected through surveys in a limited number of sites, or at low spatial resolutions—country to province levels, and processed by different methods, which are insufficient to characterize the heterogeneity of crop production. Farmers have unequal accessibilities to agricultural resources, the coarse, and identical inputs across a region tend to overstate the production in low input areas while underestimating the yield in high input land. In addition, data inaccuracy embodies in many aspects, leading to further simulated discrepancy to reported yields. For example, The SPAM yield data report higher rainfed maize yield than irrigated yield in countries such as Turkey. Nitrogen application rate is significantly and positively correlated to reported irrigated maize yields in most of maize growing reasons, indicated by an overall correlation coefficient 0.68 for the globe, whilst this correlation was small or negative in a number of African, Asian, and South American countries, such as Japan (−0.63), Pakistan (−0.13), Iran (0.00), Mexico (0.00), Zimbabwe (−0.14), and Ethiopia (−0.04). These unexpected values suggest the possible errors either with the reported yields, or with the nutrient application rates, or with other factors such as stresses which are not simulated (pests, disease, etc.), referring one of the reasons for the discrepancy between simulated and reported yields in these countries (Figure 1).

4.2 Calibration for Global Simulation

Regionalization of selected parameters has been proven to be an effective way to reduce the simulation biases, increase the spatial agreement to observation, and importantly, enhance parameters heterogeneity reflecting the actual variety of agricultural management and crop genetic characteristics [*Xiong et al*., 2014; *Folberth et al*., 2012]. However, the effectiveness of the calibration depends on the selection of parameter. In our experiment, we selected four strategies to parameterize one specific parameter, with restrictive conditions inferred from global data sets (sowing and harvesting window, reported yield, etc.) or literature, and targeting to reach the maximum spatial agreement between simulated and reported gridded yields. Within the four strategies, we found that regionalizing crop phenology (i.e., PHU) and yield correction factor (i.e.,

HI) exhibited high effectiveness in achieving better agreement than others, which is consistent with previous findings by *Angulo et al*. [2013] and *Liu et al*. [2014].

The high effectiveness of PHU and HI is because these parameters directly link to the accumulation of biomass and final allocation to yield. Their adjustments generate wide yield interval in the simulation, therefore provide a large parameter space for the calibration. As expected, tuning SD resulted in a relatively small response for simulated yields. Crop density affects crop competitions for intercepted light and nutrition, therefore modifies the actual harvest index and attainable yield in the model [*Deng et al*., 2012]. The effects caused by varying SD could be small if the crop faces other stresses such as nutrient or water, which also explains its smaller effects for maize under nonirrigation environment. For calibration of OT, our study demonstrated its limited capacity to modify simulated yield, although the yield response to temperature is sensitive to OT [*Liu et al*., 2014]. The reasons for its small role of OT are likely due to the simple structure of EPIC model. For example, optimal temperatures not only limit crop growth such as photosynthesis and growth duration, which can be modeled by the EPIC model, but also limit different growth stages and functions, such as germination, respiration, flower initiation, and induction of sterility, which are not included in the model. In part, our design for the calibration of OT may also contribute to the small effect on yield. In EPIC, the way that OT affects final yield is through the adjustment of the heat unit (PHU) absorbed each day, which requires recomputation of the PHU based on the new definition of base and optimum temperatures. In order to isolate the effect of OT, we only adjusted OT while keeping PHU and associated sowing and harvesting date as the default. This design failed to capture the overall effects from optimum temperature to final yield, likely resulted in the low effectiveness on the calibration. Nevertheless, the small effect of OT underscores the importance of parameter selection for the calibration, in some cases it may need to include multiple parameters in the calibration.

4.3. Uncertainty for Assessing the Impacts of Climate Change

Various values of parameters may cause significant differences in projected the impacts of climate change [*Angulo et al*., 2013]. By comparing the simulation outputs with different calibration strategies and various values of the parameters, our work explored and identified the calibration-induced uncertainties for estimating the impacts of climate change on global maize production. This work expands recent efforts that quantified relative contributions of various sources for crop simulation uncertainty [e.g., *Bassu et al*., 2014; *Angulo et al*., 2014], but with more explicit and aggregated information for the globe. For global maize production, the effect of climate change (under scenario of RCP 8.5 and HadEM2-ES) was strongly negative up to end of 21st century whatever parameters being used in the simulation, interpreted by accelerated phenology under higher temperatures in the future. The variability in simulated global historical yields (1981–2010) with possible values of the four parameters ranged from 3.7 $kg{\cdot}ha^{-1}$ to 9.6 $kg{\cdot}ha^{-1}$ for irrigated maize, and from 1.9 $kg{\cdot}ha^{-1}$ to 4.4 $kg{\cdot}ha^{-1}$ for rainfed maize. The predicted yields under the future climate scenario produced similar downward trends, but in general a higher simulated yield for the historical period corresponded to a smaller percentage of yield reduction for the future climate scenario. This suggests that the extent of the uncertainty of a global simulation can roughly be judged based on its ability to capture the historical crop yields. For instance, if a global EPIC simulation without calibration predicts higher historical yields, it may underestimate the negative effects of climate change, and vice versa.

Calibration resulted in varying uncertainty to estimated impact of climate change, depending on the parameters selected. Under RCP 8.5 scenario, the range for estimated change of global maize production is −5.0%∼2.2%, −15.4%∼−3.8%, and −30.0%∼−6.2%, respectively, at periods of 2020s, 2050s, and 2080. The key response of crop growth to high temperature is the shorter duration of the growing cycle, thereby decreasing radiation capture, CO_2 assimilation, and biomass and grain production [*Bassu et al*., 2014; *Tao and Zhang*, 2011]. The calibration on crop phenology leads to greater uncertainty, indicated by the widest span of projected yield change in the simulation (Figure 5 and Table 2). In contrast, estimated impacts were nearly unaffected by varying harvest index (Figure 5 and Table 2), implying less uncertainty of adjusting HI for projecting the impacts of climate change. Parameters OT and SD indirectly affected yield through PHU and HI, so the uncertainty due to adjustments of their values depends on other parameters that are adjusted simultaneously.

Our calibration in EPIC caused about 26% of uncertainty for estimating the impacts of climate change on global maize yields by the end of the 21st century, measured by the range of the estimate. Our estimate

provides the upper boundary of the uncertainty related to parameterizing specific model parameters because we examined the whole spectrum of the parameters and applied on a warmest climate change scenario (RCP8.5). The estimate could be increased if we simultaneously tuning other genotype or management parameters during the calibration. The method of regionalizing multiple parameters had been used in a few regional simulations, such as *Xiong et al*. [2014], *Folberth et al*. [2012], and *Wang et al*. [2005], in which the uncertainty may be accumulated if the simulated outputs are sensitive to more than one parameters. However, the actual uncertainty of projected impacts of climate change could be smaller than the estimate due to quality control of the input data sets and calibration procedure. For example, differences of the projected impacts for the 2080s between simulations with different calibrated parameters were around 10%, far less than the uncertainty that identified for the varying PHU (26%). In addition, simulation with an ensemble of parameters provides a surrogate of calibration. The medians of percent changes in yields across latitudes were similar in Figure 6 irrespective which parameters being adjusted. Multiple models intercomparison studies also pointed out an ensemble of model responses to climate change was similar whatever using low or high level calibration information [*Bassu et al*., 2014; *Li et al*., 2014; *Asseng et al*., 2013].

However, calibration-induced uncertainty tends to be larger at the grid scale, implying caution should be exercised when using the small scales information. This is because the inferred regional yield-climate relationship could be totally different when using different values of parameters, or choosing different calibration strategies. This is particularly true for the simulation with various PHU, indicated by the large number of grid cells (around 40%) exhibiting opposite directions of the yield-climate response. But, this grid scale information of parameter sensitivity provides important information for adaptation investment or research. On one hand, places with smaller calibration-induced uncertainty are more robust in the context of making sound adaptation investment. One the other hand, places with larger uncertainty (e.g., opposite directions of the impacts) underscores potential solutions for adaptation, such as the opposite directions of the impacts with various PHU highlight adjusting crop calendar could be an effective way to revise the negative impacts of climate change, areas with large uncertainty to OT suggest adaptation option of switching cultivars with changed optimum temperature.

5. Conclusions

Calibration is an indispensable step for crop simulation, while it is usually infeasible for the global simulation as it requests large and detailed data and intensive computation [*Ewert et al*., 2014]. The availability of a series of global data sets provided vital information to setup the global crop simulation. The EPIC simulation driven by the data sets and default model parameters roughly reproduced the spatial pattern of global maize yields of 1981–2010. Moreover, based on the data sets, performance of the simulation could be greatly improved through regionalization of selected parameters. The target for the regionalization approach was to reach the least difference between simulated and reported yields, and best spatial agreement. Regarding the estimated impacts of climate change, varying selected parameters caused minor to moderate simulation differences in percentage of predicted yield impact, with the largest of 26% up to the end of 21st century under RCP 8.5. Various settings of crop phenology tended to produce largest effect on the yield change projection, while changing harvest index had little effect on the projection. Caution should be used when applying the parameters at local scales. Adjusting parameters could result in contrasting projections in many locations, highlighting however the hotspots and potential adaptation strategies.

Acknowledgments
This research is supported by National Natural Science Foundation of China (41171093, 41471074), the Key Technologies R&D Program of China during the 12th Five-Year Plan period (2012BAC19B01), the Innovation Pillar Award (52000117), and the European Community's Seventh Framework Programme (226701). Model input data were obtained from public sources and listed in supporting information Table S1, simulation data may be obtained from WX (wei.xiong@ufl.edu). We appreciate the comments provided by three anonymous reviewers, which greatly improved the quality of this paper.

References

Angulo, C., R. Rötter, R. Lock, A. Enders, S. Fronzek, and F. Ewert (2013), Implication of crop calibration strategies for assessing regional impacts of climate change in Europe, *Agric. For. Meteorol.*, *170*, 32–40.

Angulo, C., T. Gaiser, R. Rötter, C. Børgesen, P. Hlavinka, M. Trnka, and F. Ewert (2014), 'Fingerprints' of four crop models as affected by soil input data aggregation, *Eur. J. Agron.*, *61*, 35–48.

Asseng S., et al. (2013), Uncertainty in simulating wheat yields under climate change, *Nat. Clim. Change*, *3*, 827–832.

Balkovič, J., M. van der Velde, E. Schmid, R. Skalský, N. Khabarov, N. Obersteriner, B. Sturmer, and W. Xiong (2013), Pan-European crop modeling with EPIC: Implementation, up-scaling and regional crop yield validation, *Agr. Syst.*, *120*, 61–75.

Balkovič, J., M. van der Velde, R. Skalský, W. Xiong, C. Folberth, N. Khabarov, A. Smirnov, N.D. Müeller, and M. Obersteiner (2014), Global wheat production potentials and management flexibility under the representative concentration pathways, *Global Planet. Change*, *122*, 107–121.

Bassu, S., et al. (2014), How to various maize crop models vary in their responses to climate change factors? *Global Change Biol.*, *20*, 2301–2320.
Batjes, H. N. (1995), A homogenized soil data file for global environmental research: A subset of FAO. ISRIC and NRCS profiles (version 1.0), Working Paper and Preprint 95/10b, International Soil Ref. and Inform. Cent., Wageningen, Netherlands.
Boogaart, H. L., C. A. Van Diepen, R. P. Rotter, J. M. Cabrera, and H. H. Van Laar (1998), *User's Guide for the WOFOST 7.1 Crop Growth Simulation Model and WOFOST Control Center 1.5*, technical document, 141 p., DLO Winand Staring Cent., Wageningen, Netherlands.
Challinor, A. J., T. R. Wheeler, J. M. Slingo, P. Q. Craufurd, and D. I. F. Grimes (2004), Design and optimisation of a large-area process-based model for annual crops, *Agr. For. Meteor.*, *124*(1-2), 99–120.
Challinor, A. J., J. Watson, D. B. Lobell, S. M. Howden, D. R. Smith, and N. Chhetri (2014), A meta-analysis of crop yield under climate change and adaptation, *Nat Clim. Change*, *4*(4), 287–291.
Collins, W., N. Bellouin, M. Doutriaux-Boucher, N. Gedney, T. Hinton, C.D. Jones, S. Liddicoat, and J. Martin (2008), Evaluation of the HadGEM2 model, *Met Off. Hadley Cent. Tech. Note HCTN 74*, Exeter, U. K. [Available at http://www.metoffice.gov.uk/media/pdf/8/7/HCTN_74.pdf, accessed 11 Oct 2013.]
Deng, J., J. Ran, Z. Wang, Z. Fan, G. Wang, M. Ji, J. Liu, T. Wang, J. Liu, and J.H. Brown (2012), Models and tests of optimal density and maximal yield for crop plants, *Proc. Natl. Acad. Sci. U. S. A.*, *109*, 15,823–15,828.
Deryng, D., W. J. Sacks, C. C. Barford, and N. Ramankutty (2011), Simulating the effects of climate and agricultural management practices on global crop yield, *Global Biogeochem. Cycles*, *25*, GB2006, doi:10.1029/2009GB003765.
Deryng, D., D. Conway, N. Ramankutty, J. Price, and R. Warren (2014), Global crop yield response to extreme heat stress under multiple climate change futures, *Environ. Res. Lett.*, *9*, 041001.
Elliott, J., D. Kelly, J. Chryssanthacopoulos, M. Glotter, K. Jhunjhnuwala, N. Best, M. Wilde, and I. Foster (2014), The parallel system for integrating impact models and sectors (pSIMS), *Environ. Model. Software*, *62*, 509–516.
Elliott, J., et al. (2015), The global gridded crop model intercomparison: Data and modeling protocols for Phase I (v1.0), *Geosci. Model Dev.*, *8*, 261–277.
Ewert, F., et al. (2014), Crop modelling for integrated assessment of risk to food production from climate change, *Environ. Model. Software*, *72*, 287–303.
Ewert, F., M. K. van Ittersum, T. Heckeler, O. Therond, I. Bezlepkina, and E. Andersen (2011), Scale changes and model linking methods for integrated assessment of agri-environmental systems, *Agric. Ecosyst. Environ.*, *142*, 6–17.
FAO, (1990), *Soil Units of the Soil Map of the World, FAO-UNESCO-ISRIC*, Rome.
Farr, T.G., et al. (2007), The shuttle radar topography mission, *Rev. Geophys.*, *45*, RG2004, doi:10.1029/2005RG000183.
Folberth, C., T. Gaiser, K. C. Abbaspour, R. Schulin, and H. Yang (2012), Regionalization of a large-scale crop growth model for sub-Saharan African: Model setup, evaluation, and estimation of maize yields, *Agric. Ecosyst. Environ.*, *151*(1), 21–33.
Hempel, S., K. Frieler, L. Warszawski, J. Schewe, and F. Piontek (2013), A trend-preserving bias correction – the ISI-MIP approach, *Earth Syst. Dyn. Discuss.*, *4*, 49–92.
Jones, J. W., G. Hoogenboom, C. H. Porter, K. J. Boote, W. D. Batchelor, L. A. Hunt, P. W. Wilkens, U. Singh, A. J. Gijsman, and J. T. Ritchie (2003) The DSSAT cropping system model, *Eur. J. Agron.*, *18*, 235–265.
Keating, B. A., et al. (2003) An overview of APSIM, a model designed for farming systems simulation, *Eur. J. Agron.*, *18*, 267–288.
Li, T., et al. (2014) Uncertainties in predicting rice yield by current crop models under a wide range of climatic conditions, *Global Change Biol.*, *21*, 1328–1341.
Liu, J. (2009), A GIS-based tool for modeling large-scale crop-water relations, *Environ. Model. Software*, *23*(3), 411–422.
Liu, J. G., J. R. Williams, A. J. B. Zehnder, and H. Yang (2007), GEPIC: Modelling wheat yield and crop water productivity with high resolution on a global scale, *Agric. Syst.*, *94*, 478–493.
Liu, M., B. He, A. Lu, L. Zhou, and J. Wu (2014), Parameters sensitivity analysis for a crop growth model applied to winter wheat in the Huanghuaihai Plain in China, *Geosci. Model Dev. Discuss.*, *7*, 3867–3888.
Lychuk, T. E., R. C. Izaurralde, R. L. Hill, W. B. McGill, and J. R. Williams (2014), Biochar as a global change adaptation: Predicting biochar impacts on crop productivity and soil quality for a tropical soil with the Environmental Policy Integrated Climate (EPIC) model, *Mitig. Adapt. Strat. Global Change*, *20*, 1437–1458.
Monfreda, C., N. Ramankutty, and J. A. Foley (2008), Farming the planet: 2. Geographic distribution of crop areas, yields, physiological types, and net primary production in year 2000, *Global Biogeochem. Cycles*, *22*, GB1022, doi:10.1029/2007GB002947.
Müeller, N. D., J. S. Gerber, M. Johnston, D. K. Ray, N. Ramankutty, and J. A. Foley (2012), Closing yield gaps through nutrient and water management, *Nature*, *490*, 254–257.
Rosenzweig, C., et al. (2013), The agricultural model intercomparison and improvement project (AgMIP): Protocols and pilot studies, *Agric. For. Meteorol.*, *170*, 166–182.
Rosenzweig, C., et al. (2014), Assessing agricultural risks of climate change in the 21st century in a global gridded crop model intercomparison, *Proc. Natl. Acad. Sci. U. S. A.*, *111*, 3268–3273.
Sacks, W. J., D. Derying, J. A. Foley, and N. Ramankutty (2010), Crop planting dates: An analysis of global patterns, *Global Ecol. Biogeogr.*, *19*, 607–620.
Schaap, M. G., and W. Bouten (1996), Modelling water retention curves of sandy soils using neural networks, *Water Resour. Res.*, *32*, 3033–3040.
Sheffield, J., G. Goteti, and E. F. Wood (2006), Development of a 50-year high-resolution global dataset of meteorological forcings for land surface modeling, *J Clim.*, *19*, 3088–3111.
Tao, F., and Z. Zhang (2011), Impacts of climate change as a function of global mean temperature: Maize productivity and water use in China, *Clim. Change*, *105*, 409–432.
Tatsumi, K., Y. Yamashiki, V. S. Roverto, K. Takara, Y. Matsuoka, I. Takahashi, K. Maruyama, and N. Kawahara (2011), Estimation of potential changes in cereals productions under climate change scenarios, *Hydrol. Processes*, *25*(17), 2715–2725.
Van Wart, J., K. C. Kersebaum, S. Peng, M. Milner, and K. G. Cassman (2013), Estimating crop yield potential at regional to national scales, *Field Crops Res.*, *143*, 34–43.
Waha, K., L. G. J. Van Bussel, C. Muller, and A. Bondeau (2012), Climate-driven simulation of global crop sowing dates, *Global Ecol. Biogeogr.*, *21*(2), 247–259.
Wang, X., X. He, J. R. Williams, R. C. Izaurralde, and J. D. Atwood (2005), Sensitivity and uncertainty analysis of crop yields and soil organic carbon simulated with EPIC, *Trans. ASAE*, *48*(3), 1041–1054.
Wang, X., R. D. Harmel, J. R. Williams, and W. L. Harman (2006), Evaluation of EPIC for assessing crop yield, runoff, sediment and nutrient losses from watersheds with poultry litter fertilization, *Trans. ASABE*, *49*(1), 47–59.

Williams, J. R. (1995), The EPIC model, in *In Computer Models of Watershed Hydrology*, edited by V. P. Singh, pp. 909–1000, Water Resour. Publ., Highlands Ranch, Colo.

Xiong, W., I. Holman, D. Conway, E. Lin, and Y. Li (2008), A crop model cross calibration for use in regional climate impacts studies, *Ecol. Modell.*, *213*, 365–380.

Xiong, W., J. Balkovic, M. van der Velde, Z. Zhang, R.C. Izaurralde, R. Skalsky, E. Lin, N. Mueller, and M. Obersteiner (2014), A calibration procedure to improve global rice yield simulations with EPIC, *Ecol. Modell.*, *273*, 128–139.

You, L., and S. Wood (2006), An entropy approach to spatial disaggregation of agricultural production, *Agric. Syst.*, *90*, 329–347.

You, L., S. Crespo, Z. Guo, J. Koo, W. Ojo, K. Sebastian, M. T. Tenorio, S. Wood, and U. Wood-Sichra (2009), *Spatial Production Allocation Model (SPAM) 2000*, version 3 Release 2, IFPRI, Washington D. C. [Available at http://MapSPAM.info.]

Zhang, X., R. C. Izaurralde, D. H. Manowitz, R. Sahajpal, T. O. West, A. M. Thomson, M. Xu, K. Zhao, S. D. LeDuc, and J. R. Williams (2015), Regional scale cropland carbon budgets: Evaluating a geospatial agricultural modeling system using inventory data, *Environ. Modell. Software*, *63*, 199–216.